

Excitation Energy Transfer in Dimeric Light Harvesting Complex I: A Combined Streak-Camera/Fluorescence Upconversion Study

Bas Gobets,^{*,†} John T. M. Kennis,[‡] Janne A. Ihalainen,[§] Michela Brazzoli,^{||} Roberta Croce,^{||} Ivo H. M. van Stokkum,[†] Roberto Bassi,^{||} Jan P. Dekker,[†] Herbert van Amerongen,[†] Graham R. Fleming,[‡] and Rienk van Grondelle[†]

Division of Physics and Astronomy of the Faculty of Sciences, Vrije Universiteit, De Boelelaan 1081, 1081 HV Amsterdam, The Netherlands, Department of Chemistry, University of California, and Physical Biosciences Division, Lawrence Berkeley National Laboratory, Berkeley, California 94720-1460, Department of Chemistry, University of Jyväskylä, P.O.Box 35, FIN-40351, Jyväskylä, Finland, and Facoltà di Scienze MM. FF.NN., Università di Verona, Strada Le Grazie- Cà Vignal, 37134 Verona, Italy

Received: May 17, 2001; In Final Form: July 25, 2001

The excitation dynamics in isolated dimers of light harvesting complex I, the peripheral light harvesting complex associated with photosystem I in green plants, was studied by time-resolved fluorescence spectroscopy. A unique combination of two techniques, fluorescence upconversion and synchroscan streak-camera measurements, revealed the energy transfer and decay of excitations over a time range from a hundred femtoseconds up to several nanoseconds, over a spectral range from 570 to 780 nm. Energy transfer from initially excited carotenoid S₂ states to the chlorophylls was found to occur within 0.15 ps. Energy transfer from chlorophyll *b* (Chl*b*) to chlorophyll *a* (Chl*a*) occurred with two distinctly different lifetimes of 0.5 and 2–3 ps. The 0.5 ps component mainly reflects transfer to bulk Chl*a*, whereas the 2–3 ps component may also account for direct transfer to the special red-shifted Chl*a* forms. Equilibration between the bulk Chl*a*'s and these red-shifted forms occurs with lifetimes of 4–8 and ~20 ps, which are assigned to intra- and intermonomer equilibration, respectively. After completion of the energy transfer processes, the fluorescence decays biexponentially. The largest fraction of excitations (75–80%) decays with a 3 ns time constant, which is attributed to both the Lhca1/Lhca4 heterodimer and a homodimer of either Lhca2 or Lhca3, whereas the remaining fraction, which decays in 0.6 ns, is assigned to the remaining homodimer. A comparison is made between the kinetics of LHCI and the more well studied CP29 and LHCII light harvesting complexes of photosystem II, which belong to the same family of Lhca/*b* light harvesting proteins, but do not feature the unique red-shifted Chl*a* forms which are found in LHCI.

Introduction

Photosystem I (PSI) consists of a core complex containing both the PSI reaction center and a core antenna consisting of 90–100 chlorophyll *a* (Chl*a*) molecules. In green plants a peripheral antenna complex, light harvesting complex I (LHCI),¹ is attached to the core complex. LHCI binds another 80–100 antenna chlorophylls, both Chl*a* and chlorophyll *b* (Chl*b*).^{1,2} Consequently, about 170–200 chlorophylls are contained in one PSI unit, which is therefore designated PSI-200. LHCI consists of four different proteins, Lhca1–4, which have molecular masses ranging from 20 to 24 kDa, and which are thought to be present in approximately equal amounts.¹ Lhca1 and Lhca4 have been shown to form a heterodimer,^{3,4} which at 77 K exhibits a red-shifted steady-state emission maximum at 730 nm,¹ and is therefore designated LHCI-730. The 730 nm emission may originate either from red-shifted Chl*a* located in Lhca4⁵ or from pigment–pigment interaction induced upon dimerization.⁶ Similar red-shifted Chl*a* forms are also found in PSI core complexes and have also been suggested to result from dimers or larger aggregates of Chl*a*.^{7,8}

Biochemical data suggest that Lhca2 and Lhca3 assemble as homodimers rather than heterodimers.³ The 77 K fluorescence of these complexes has usually been reported to peak at 680 nm, and has therefore so far been designated LHCI-680.¹ It has recently been suggested, however, that the 680 nm form represents monomeric Lhca2 and Lhca3, rather than dimers of these proteins which represent the functional complexes *in vivo*.⁶ This idea is corroborated by recent low temperature (5 K) spectroscopy data of dimeric LHCI, which instead of a 680 nm emitter show the presence of an emission band at ~702 nm (F702) in addition to the F730 band. It was suggested that F702 arises from an absorption band peaking at ~695 nm, and that Lhca2/Lhca3 homo/heterodimers are responsible for this band.²

So far it has not been possible to isolate the Lhca2/3 proteins from the Lhca1/4 heterodimers without breaking up the native dimers.

Electron microscopy data indicated that in total about 3–4 LHCI dimers bind to the PSI core complex near the PSI-F and PSI-J subunits.⁹

Measurements of the pigment-to-protein stoichiometry indicated that each LHCI monomer contains 10 Chl molecules, of which 8 are Chl*a* and 2 are Chl*b*.⁶ Besides the Chl's, each LHCI monomer also contains two carotenoid (Car) molecules in a mixture of violaxanthin, lutein, and β -carotene.⁶

* Corresponding author. Fax: +31 20 4447899. E-mail: bas@nat.vu.nl.

[†] Vrije Universiteit.

[‡] University of California.

[§] University of Jyväskylä.

^{||} Università di Verona.

TABLE 1: Lifetimes Observed in LHCI, LHCII, and CP29

experiment	Car (S ₂) decay	Chlb–Chla transfer		Chla equilibration		decay	
		fast	slow	fast	slow	fast	slow
Car excitation (UPC)	0.14 ps	0.5 ps					
Chlb excitation (UPC)		0.5 ps	4 ps	4 ps			
Chlb excitation (UPC + streak)	0.3 ps	0.3 ps	3.6 ps	3.6 ps	20 ps	0.6 ns	3 ns
Chla excitation (streak camera)		0.5 ps		8 ps	18 ps	0.6 ns	3 ns
concluding	~0.14 ps	0.5 ps	2–3 ps	4–8 ps	~20 ps	0.6 ns	3 ns
Melkozernov et al. ((r-)LHCI-730) ^{5,17}		0.5–0.6 ps		5 ps	30–50 ps	several, 0.3–7 ns	
LHCII monomers (77 K) ^{12–14}	0.1 ps	0.2 ps	3 ps	0.3 ps, 0.45 ps, 5 ps, 12 ps, 18 ps			2.9 ns
CP29 (77 K) ^{11,12}	70–90 fs	0.35 ps	2.2 ps	280 fs	10–13 ps		

The pigment stoichiometry of LHCI is almost the same as that found for CP29, an antenna protein of photosystem II. The LHCI proteins show a high sequence homology with CP29, as well as with other plant light harvesting proteins,¹ such as those of LHCII, the only one of the Lhca/b proteins of which a structure (at 3.4 Å) has been resolved.¹⁰

The main function of these light harvesting proteins is to absorb light and to transfer the collected energy to the reaction center of either PSI or PSII. A unique property of LHCI is the presence of the above-mentioned red-shifted Chla forms, which absorb around 695–705 nm,^{1,2} and which are expected to have a pronounced influence on the energy transfer dynamics. In contrast to LHCII and CP29, which have been studied extensively by femtosecond time-resolved spectroscopy,^{11–14} energy transfer processes in LHCI have not been studied in much detail so far. Early experiments by Pålsson et al.¹⁵ and Mukerji et al.¹⁶ suffer from a limited time resolution, and were performed on LHCI preparations that were not very well defined. Recently, Schmid et al.⁴ succeeded in overexpression of Lhca1 and Lhca4 in *E. coli*, and in the reconstitution of these proteins with chlorophylls and carotenoids. A heterodimer LHCI-730 was generated, which quite closely resembled the native dimer. Time-resolved absorption and fluorescence emission experiments performed on these reconstituted Lhca4 monomers and LHCI-730 dimers¹⁷ revealed a ~5 ps energy transfer component within the Chla band. A second ~30 ps energy transfer component was observed only in the dimer.^{5,17} It was concluded that these two components correspond to intra- and intermonomer energy transfer between the bulk Chla and the red-shifted Chla forms, respectively. A fast 0.5–0.6 ps component was assigned to Chlb to Chla transfer.¹⁷ The decay of excitations in both reconstituted and native LHCI-730 was found to be multiexponential with major ~280 and 800–850 ps components and a small 2–2.5 ns contribution⁵ (see Table 1).

In this contribution, we present room-temperature time-resolved fluorescence data of a well-defined LHCI preparation¹⁸ containing all the (native) LHCI dimers. The combination of fluorescence upconversion and streak-camera data provides both a high time resolution (~0.1 ps) and the complete spectral evolution in the 570–780 nm wavelength interval. Energy transfer kinetics were recorded for preferential excitation of the carotenoids, Chlb, and Chla.

Materials and Methods

Sample. Dimeric LHCI was isolated from maize as a mixture of dimers of all four Lhca1–4 proteins, using β-DM and sucrose gradient centrifugation as described in ref 18. Size exclusion chromatography, nondenaturing gel electrophoresis, density gradient ultracentrifugation, and cross-linking experiments all confirmed that the preparation indeed consisted of dimers only.⁶ The preparation was treated with antibodies against all four Lhca proteins, which clearly indicated that all four were present. No

impurities were detected by SDS–PAGE. The Chla to Chlb ratio in this preparation was 3.6–3.8.

Streak-Camera Measurements. The sample was diluted with a buffer containing 10 mM Tricine (pH 7.5), 0.5 M sucrose, and 0.03% w/v dodecyl-β-D-maltoside to an optical density (OD) of 0.12 per 3 mm at the Q_y absorption maximum.

The sample, contained in a spinning cell (optical path length = 3 mm), was excited with 100 fs pulses of 400 nm (Chla excitation) or 470 nm (Chlb excitation) which were generated at a 125 kHz repetition rate using a titanium:sapphire based oscillator (Coherent MIRA), a regenerative amplifier (Coherent REGA), and a double pass optical parametric amplifier (Coherent OPA-9400). The applied pulse energy was typically 4 nJ, sufficiently low to avoid singlet–singlet annihilation. Fluorescence was collected at right angle to the excitation beam using achromatic lenses, and detected through a sheet polarizer set at magic angle (54.7°), with a Hamamatsu C5680 synchroscan streak camera and a Chromex 250IS spectrograph.

The streak images were recorded on a Hamamatsu C4880 CCD camera which was cooled to –55 °C.

The streak images measure 315 nm in the spectral domain (1018 pixels, spectral resolution 8 nm) and either 200 ps or 2.2 ns (1000 pixels) in the time domain. The full width at half-maximum (fwhm) of the time response of this system was 3–3.5 ps for the 200 ps time range and ~20 ps for the 2.2 ns time range. For more details on the data acquisition and processing we refer to Gobets et al.¹⁹

Fluorescence Upconversion Measurements (UPC). The OD₆₈₀ of the sample was 0.3/mm. The sample was pumped through a flow cell (1 × 1 mm) and was thermostated at 10 °C.

The fluorescence upconversion experiments were performed basically as described by Walla et al.²⁰ Briefly, excitation pulses at 510 nm (Car excitation) and 470 nm (Chlb excitation) were generated at a 250 kHz repetition rate, using a laser system similar to the one described above. At this repetition rate a given sample volume was exposed to about 25 successive laser pulses during the time it moved through the laser focus. The excitation pulse energy was typically 8 nJ. A part of the amplified 800 nm pulses was used as the gate beam. The excitation pulses were focused into the flow cell, which was placed at one focus of an elliptical mirror. The fluorescence of the sample was collected by the ellipsoid and focused into a 0.5 mm BBO crystal placed at the other focus. Here the fluorescence was mixed with the gate beam to create the upconversion signal. The polarization angle between the excitation light and the gate beam was adjusted to magic angle (54.7°) using a broad-band variable wave plate (CVI) which was placed in the excitation beam.

A double monochromator was used to select a ~8 nm bandwidth spectral window from the upconversion signal, which was detected with a photomultiplier. For Chlb excitation, detection was at 655 nm (Chlb), 695 nm (bulk Chla), and 723

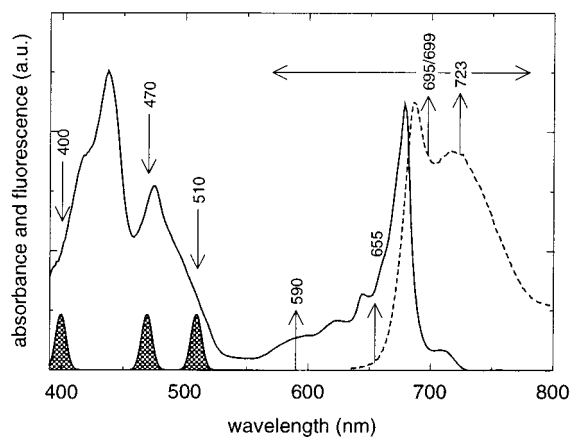


Figure 1. The 5 K absorption spectrum (solid) and RT steady-state emission spectrum (dashed) of the isolated dimeric LHCI particles. Arrows pointing down indicate excitation wavelengths of the time-resolved fluorescence experiments (400, 470, and 510 nm). Representative spectral profiles of the excitation pulses have been indicated. Arrows pointing up indicate detection wavelengths of the fluorescence upconversion experiments (591, 655, 695/699, and 723 nm). The horizontal double arrow indicates the fluorescence detection range of the streak-camera experiments that was analyzed (575–775 nm).

nm (red Chla). For Car excitation, detection was at 591 nm (Car S_2), 655 nm (Chlb), and 699 nm (bulk Chla). The cross-correlation between pump and gate pulse was 280–300 fs.

Data Analysis. For both 400 and 470 nm excitation the upconversion traces at three detection wavelengths were analyzed simultaneously, independently of the streak-camera data.

The streak-camera measurements were analyzed using a model with parallel decaying components, which yields decay associated spectra (DAS). For 400 nm excitation both the 200 ps and 2.2 ns time range data were analyzed simultaneously, and for 470 nm excitation the streak data of both time ranges were analyzed simultaneously with the upconversion data for that wavelength of excitation. The amplitude of both upconversion and streak-camera traces obtained for the 200 ps time range were scaled to the streak data obtained for the 2.2 ns time range. Since we did not apply direct excitation of the Chl Q_y transitions, the analysis was performed under the condition that no fluorescence was present above 665 nm at time zero. The results of the simultaneous fitting were compared to separate fits of the data obtained for the different time ranges. In all cases the instrument response function was assumed to be a Gaussian, the width of which was a free parameter of the fit. All the DAS shown were corrected for the spectral sensitivity of the apparatus.

Results

Steady-State Absorption and Emission Spectrum. The 5 K absorption spectrum of LHCI in Figure 1 (solid line) reveals the different absorption bands of the chromophores present in the system. In the blue part of the spectrum the Soret bands of Chla and Chlb peak at 438 and 475 nm, respectively.^{2,16,21} The Chlb Soret absorption band overlaps strongly with absorption due to the S_2 transition of the carotenoids (400–525 nm).^{2,21} The maximum at 643.5 nm is assigned to a Chlb Q_y transition,^{2,11,16,21,22} and a second Chlb band with a maximum at 650 nm was resolved from linear dichroism measurements,² indicating that at least two spectroscopically distinct Chlb binding sites are present in LHCI, similar to CP29.^{11,12} The Q_y region of Chla peaks at 678.5 nm, and exhibits a weak shoulder around 671 nm. The red-shifted Chla forms are represented by a broad band around 710 nm.

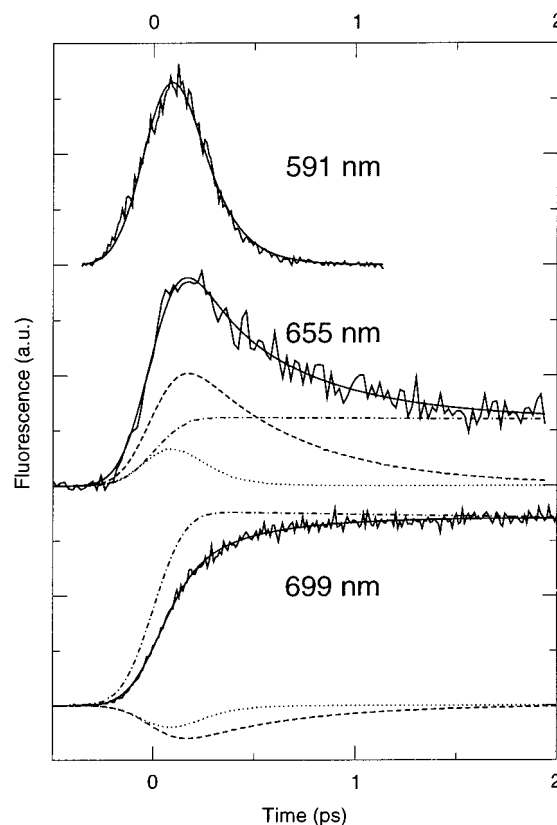


Figure 2. RT, 510 nm excitation upconversion traces of isolated LHCI detected at 591, 655, and 699 nm (noisy solid), the result of the simultaneous fit (solid), and the 0.14 ps (dotted), 0.5 ps (dashed), and long-lived (dot-dashed) lifetime contributions to the fit.

The wavelengths of excitation used in the time-resolved experiments have been indicated in Figure 1 by arrows pointing down. The room-temperature absorption spectrum was decomposed using (shifted) room-temperature absorption spectra of Chla (maximum at 440 nm) and Chlb (maximum at 475 nm) in acetone (not shown), to roughly estimate the extent of selectivity for the various pigments for these wavelengths of excitation. Chla and Car were excited quite selectively using 400 nm (~90% Chla) and 510 nm light (~80% Car), respectively. It was not possible to achieve such selective excitation of Chlb; using 470 nm light about 50% Chlb, 45% Car and 5% Chla are excited. Figure 1 also shows the room-temperature steady-state emission spectrum for excitation at 455 nm. This emission spectrum exhibits a sharp maximum at 686 nm, due to the emission of the bulk Chla molecules, and a broad sideband with a maximum around 720 nm due to the emission by the red-shifted Chla species. The wavelengths of detection used in the fluorescence upconversion experiments are indicated in Figure 1 by the arrows pointing up: at 591 nm for emission of the carotenoids, at 655 nm for the emission of Chlb, at 695–699 nm for the emission of bulk Chla, and at 723 nm for the emission of the red-shifted Chla forms. The analyzed fluorescence detection range of the streak-camera is indicated by the horizontal double arrow.

Time-Resolved Fluorescence for Carotenoid Excitation. In Figure 2, upconversion traces are shown for preferential excitation of the carotenoid molecules at 510 nm detected at 591, 655, and 699 nm. Three lifetimes (0.14 ps, 0.5 ps, and long-lived) were needed to simultaneously fit the three recorded traces. The decay of the fluorescence at 591 nm, representing carotenoid S_2 fluorescence, is very fast. In a free fit, the fastest (0.14 ps) component dominates the fluorescence decay at this

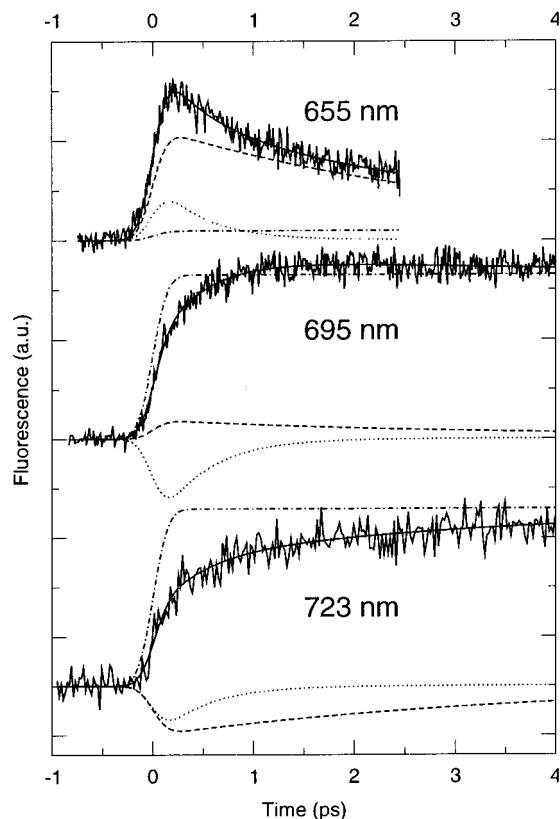


Figure 3. RT, 470 nm excitation upconversion traces of isolated LHCI detected at 655, 695, and 723 nm (noisy solid), the result of the simultaneous fit (solid), and the 0.5 ps (dotted), 4 ps (dashed), and long-lived (dot-dashed) lifetime contributions to the fit.

wavelength. Forcing the amplitudes of the other two components of the fit to zero for this wavelength did not change the quality of the total fit (Figure 2). Therefore, we conclude that practically all carotenoid S_2 fluorescence decay (by energy transfer or internal conversion) occurs with the 0.14 ps time constant.

For detection at 655 nm, the 0.14 ps component only has a small (positive) contribution, reflecting the tail of the carotenoid fluorescence. At 699 nm the contribution of the 0.14 ps component is negative, indicating energy transfer from the carotenoids to Chl a , although a small part of this ingrowth may also be attributed to Soret- Q_y relaxation of the small fraction of directly excited Chl a 's.

The 0.5 ps component represents the largest decay component of fluorescence at 655 nm (primarily Chl b). This component is negative at 699 nm and is therefore attributed to Chl b -Chl a transfer.

The long-lived component has a positive amplitude at both 655 and 699 nm and accounts for all slow components.

Time-Resolved Fluorescence for Chlorophyll b Excitation.

In Figure 3, the upconversion traces are shown for excitation at 470 nm, which is about 50% selective for Chl b , detected at 655, 695, and 723 nm. Three lifetimes are needed to simultaneously fit the three traces. The shortest lifetime found is 0.5 ps. The amplitude of this component is positive at 655 nm and negative both at 695 and 723 nm, indicating that this component reflects energy transfer from Chl b to Chl a . The time constant matches the 0.5 ps transfer component found for 510 nm excitation (see above).

The second component has a lifetime of 4 ps and shows a positive amplitude at both 655 and 695 nm, and a negative amplitude at 723 nm, indicating that this component reflects energy transfer from both Chl a and Chl b to the red Chl a forms,

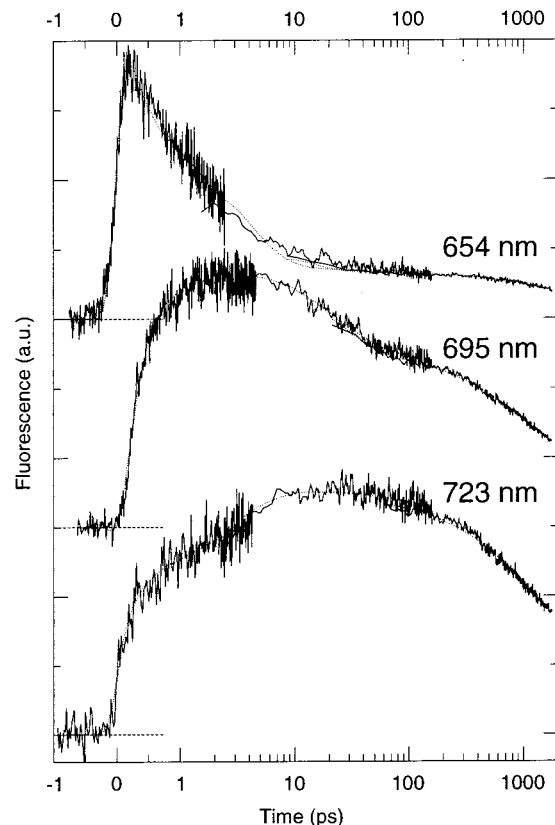


Figure 4. RT combined 470 nm excitation traces of isolated LHCI of the upconversion experiments and the 200 ps and 2.2 ns time range streak-camera experiments (solids) and the simultaneous fit (dotted). The scaling of the time axis is linear from -1 to 1 ps and logarithmic above 1 ps. The streak-camera traces have been plotted from $t \sim 2$ ps and ~ 20 ps for the 200 ps and 2.2 ns time range, respectively.

although it cannot be ruled out that Chl b in fact transfers to bulk Chl a (see below). The remaining dynamics takes place on a time scale that extends beyond the range of the fluorescence upconversion experiments, and is accounted for by the third, long-lived component which exhibits a positive amplitude for all three wavelengths of detection.

Time-resolved fluorescence for Chl b (470 nm) excitation was also recorded with the streak-camera setup. The streak-camera measurements provide the dynamics over the whole 570-780 nm wavelength range in the picosecond to nanosecond time range. Subpicosecond processes can be observed as well, but due to the relatively broad instrument response, the time constants of these processes cannot be determined very precisely from these experiments alone. By performing a simultaneous global analysis of the streak data at the 200 ps and 2.2 ns time ranges together with the three upconversion traces recorded for 470 nm excitation, lifetimes of hundreds of femtoseconds to several nanoseconds (4 orders of magnitude in time) could be determined accurately. Figure 4 displays the traces recorded at the three wavelengths of detection for which the upconversion and streak-camera measurements were combined. It demonstrates that the traces recorded with different experimental techniques join smoothly (note that the traces are plotted on a linear-logarithmic scale).

The decay associated spectra resulting from the global analysis are shown in Figure 5. We note that the results of the simultaneous analysis are in agreement with the results obtained for separate analyses of the individual time ranges (not shown).

The fastest component of the simultaneous analysis is fitted with a 0.3 ps time constant. The corresponding DAS (solid) is

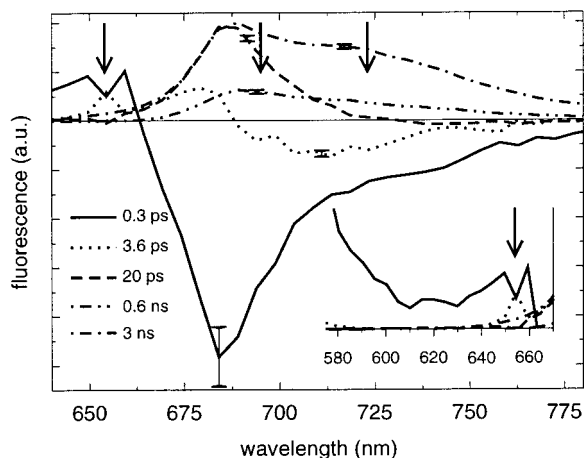


Figure 5. Decay associated spectra of fluorescence decay of isolated LHCI for 470 nm excitation: 0.3 ps (solid), 3.6 ps (dotted), 20 ps (dashed), 0.6 ns (double-dot-dashed), and 3 ns (dot-dashed). The inset shows a blowup of the 575–670 nm detection region. The arrows show the wavelengths of the upconversion traces that were fitted simultaneously with the streak-camera data. Rough error bars have been included at selected wavelengths.

positive in the carotenoid emission region (570–630 nm, see inset), shows a maximum around 645–650 nm in the Chl*b* region, and exhibits a negative band in the main-band Chl*a* region. A DAS that is positive in one region of the spectrum and negative in another is characteristic for energy transfer between two spectrally different chromophores. We therefore assign this component to energy transfer from the carotenoids (which are receiving a significant fraction of the excitations for 470 nm excitation) and Chl*b* to the bulk Chl*a*. The tail of the rise in the fluorescence above 700 nm is somewhat higher than would be expected for bulk Chl's, suggesting that a small fraction of the energy transfer from the carotenoid may be directed to the red-shifted Chl*a*'s.

The ~ 0.3 ps time constant may in fact represent a mixture of the ~ 0.14 ps carotenoid to Chl*a* component (Figure 2) and the ~ 0.5 ps Chl*b* to Chl*a* component (Figures 2 and 3) observed in the separate fits of the fluorescence upconversion experiments.

The second component in Figure 5 exhibits a 3.6 ps time constant. The DAS of this component (dotted) shows maxima at 655 nm (Chl*b*) and 680 nm (bulk Chl*a*), and is negative above 687 nm with a broad minimum around 715 nm. This component represents two energy transfer processes: both from the bulk Chl*a* to a red-shifted Chl*a* form and from Chl*b* to either the bulk Chl*a* or the red-shifted Chl*a* form. In view of the 678 nm bulk absorption maximum, the 680 nm emission must result from a relatively blue fraction of the bulk Chl's, possibly the Chl's corresponding to the shoulder around 671 nm. We do note that there is a slight discrepancy between the streak-camera data and the upconversion trace at 655 nm, apparent from the "dip" in the 0.3 ps DAS and the peak in the 3.6 ps DAS at this wavelength, which probably results from the uncertainty in the estimation of the instrument response of the streak camera.

The lifetime of the third component is about 20 ps, and it exhibits a DAS (dashed) which shows a pronounced peak at 686 nm, and which drops below zero only slightly above ~ 730 nm. This component represents slow transfer from bulk Chl*a* to a red-shifted Chl form, and may be attributed to intermonomer transfer within a dimer.⁵ Obviously, the DAS shows a much larger positive area as compared to the negative area, which suggests that either some loss of excitations occurs as well during the 20 ps process, or that the red-shifted state has a lowered oscillator strength, i.e., is somewhat forbidden.

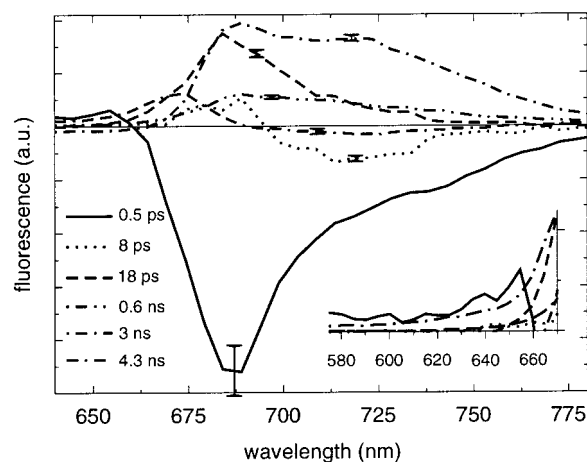


Figure 6. Decay associated spectra of fluorescence decay of isolated LHCI for 400 nm excitation: 0.5 ps (solid), 8 ps (dotted), 18 ps (dashed), 0.6 ns (double-dot-dashed), 3 ns (dot-dashed), and 4.3 ns (dot-long dashed). The inset shows a blowup of the 575–670 nm detection region. Rough error bars have been included at selected wavelengths.

The final two processes which take place with 0.6 and 3 ns time constants are represented by all-positive decay associated spectra (double-dot-dashed and dot-dashed) and account for the decay of excitations after the energy transfer processes are completed.

Time-Resolved Fluorescence for Chlorophyll *a* Excitation.

In Figure 6 the decay associated spectra resulting from the simultaneous global analysis of the 200 ps and 2.2 ns time range streak measurements for 400 nm excitation are shown. At this wavelength of excitation mainly Chl*a* is excited. The results of the simultaneous fit are consistent with the results obtained for fits of the individual time ranges (not shown).

The fastest component is fitted with a 0.5 ps time constant. The DAS of this component (solid) exhibits a (slightly) positive Chl*b* region, which peaks at 655 nm and is negative in the bulk Chl*a* region with a minimum around 686 nm. We assign this component to both energy transfer from the small fraction of Chl*b* that is excited at 400 nm to Chl*a*, and Chl*a* Soret to Q_y relaxation. The observation that the DAS has virtually no amplitude in the carotenoid region indicates that indeed no significant amount of carotenoids is excited at 400 nm. Although the 0.5 ps lifetime corresponds very well to the Chl*b* to Chl*a* transfer times reported above, we note that in the absence of upconversion data for 400 nm excitation we cannot accurately determine this time constant.

The second component corresponds to a 8 ps time constant and exhibits a spectrum (dotted) which shows maxima at ~ 680 and ~ 690 nm and a negative region in the red wavelength region with a minimum around 719 nm. The negative part of this spectrum is very similar to that of the 3.6 ps transfer component observed for 470 nm excitation (see above); however, the positive part, reflecting decay of "bulk" emission, is about ~ 10 nm red-shifted with respect to the corresponding decay in the DAS for 470 nm excitation. Also, the emission of Chl*b* is almost absent for 400 nm excitation, which implies that the Chl*b* responsible for the slow Chl*b* to Chl*a* energy transfer is not excited at 400 nm. The differences in time constants between the 3.6 ps component found for 470 nm excitation and the 8 ps time constant found for 400 nm excitation suggests that the former represents a mixture of a 2–3 ps Chl*b* to *a* transfer component and (a) slower 4–8 ps bulk Chl*a* to red-shifted Chl*a* component(s) (see below).

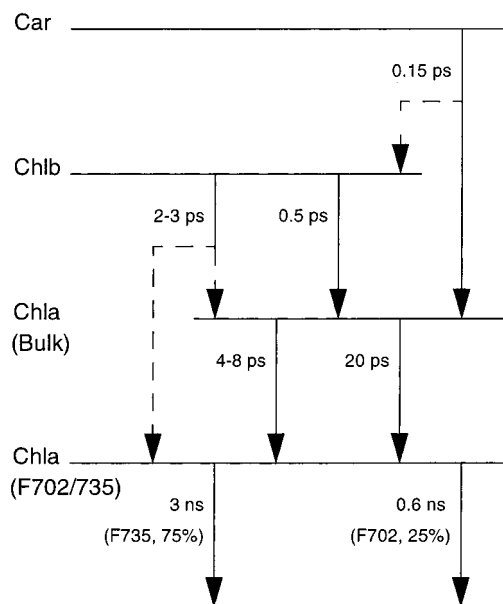


Figure 7. Scheme of energy transfer pathways in LHCI. Dashed lines indicate pathways which presently cannot be decided upon based on our data (see discussion).

The third component, which is fitted with a 18 ps time constant, closely resembles the 20 ps component observed in the analysis of the 470 nm excited data. Therefore, although there is no real negative region in the red part of the spectrum (dashed), we also assign this component to energy transfer from bulk Chla to a red-shifted Chla form, maybe combined with some decay of excitations.

The 0.6 ns and 3 ns component (double-dot-dashed and dot-dashed) are basically identical with those found for excitation at 470 nm. A small 4.3 ns component (dot-long-dashed) which peaks around 675 nm accounts for some free Chla present in the preparation.

Discussion

We summarize our results in the scheme presented in Figure 7. We note that this scheme should be regarded as a summary of the observed lifetimes rather than as a true kinetic scheme, since no backward (uphill) rates have been included and no explicit separation is made between the different Lhca1–4 dimers. The lifetimes obtained in the different experiments and their assignments are summarized in Table 1. For comparison, results obtained by Melkozernov et al. for (reconstituted) LHCI-730^{5,17} as well as results obtained for LHCI and CP29 are also listed in Table 1.

Carotenoid to Chlorophyll *a* Transfer. Fast energy transfer from the carotenoid S_2 state to Chla occurs within about 0.15 ps. This time constant is in the range of fluorescence lifetimes of carotenoids in organic solvents, which is about 0.12–0.18 ps for β -carotene²³ and ~ 0.32 ps for violaxanthin,²⁴ and carotenoid S_2 lifetimes found in LHCI, CP29,¹² and the PSI core complex.²⁵ Our data do not permit determination of the Car to Chl transfer efficiency, but steady-state fluorescence excitation measurements performed on the same LHCI preparations indicate that this efficiency is at least 80% (Ihalainen et al., unpublished results). For both LHCI and CP29 the overall efficiency of Car to Chl transfer was also estimated to be approximately 80%, which included 15–20% transfer via the Car S_1 state occurring on a ~ 1 ps time scale.¹² Although our data on LHCI do not reveal a second, slower, Car to Chl transfer

component, we cannot rule out that a fraction of the Car to Chl transfer in LHCI is mediated by the S_1 state.

Carotenoid to Chlorophyll *b* Transfer. It is unclear if Car transfers directly to Chlb in LHCI. The biexponential ingrowth at 699 nm upon carotenoid excitation (Figure 2) shows a larger amplitude for the 0.5 ps rise attributed to Chlb to Chla transfer than for the 0.14 ps Car to Chl transfer component. This may be an indication that direct Car to Chlb transfer occurs (followed by Chlb to Chla transfer), since the amount of Chlb that is directly excited at 510 nm is expected to be 10-fold lower than the amount of Car which is excited at that wavelength. On the other hand, if Car to Chlb transfer occurs, the 0.14 ps component is expected to show a negative amplitude for 655 nm detection, since at this wavelength the ingrowth of Chlb fluorescence would be larger than the corresponding decay of carotenoid fluorescence. Since the 0.14 ps component shows a positive (decay) amplitude at 655 nm, this argues against Car to Chlb transfer.

In CP29 the carotenoids transfer exclusively to Chla, in contrast to LHCI in which energy transfer from neoxanthin to Chlb occurs.¹² We note that LHCI contains three carotenoids per monomer, in contrast to the two Car's that are present in both LHCI and CP29, and that LHCI does not contain neoxanthin. Therefore, LHCI is more likely to resemble CP29 in this respect.

Chlorophyll *b* to Chlorophyll *a* Transfer. Fast transfer from Chlb to Chla occurs in 0.5 ps and does not, most likely, involve a significant amount of transfer to the red Chla forms. A similar 0.5–0.6 ps Chlb to Chla transfer component was observed in a transient absorption study of reconstituted monomeric Lhca4 polypeptides.¹⁷ Upon Chlb excitation a 3.6 ps process is observed that involves a decay in both the Chlb region and the bulk Chla region, and a rise in the red Chla region. Upon excitation of Chla (Figure 6) a similar component is present, which, however, lacks the decay in the Chlb region, and which is associated with a slower, 8 ps, lifetime. This suggests that the observed 3.6 ps component in the global analysis of the Chlb excited streak measurements represents a mixture of both a 2–3 ps Chlb to (red) Chla transfer component and (a) slower bulk Chla to red Chla transfer component(s) (see also below). This idea is further supported by a separate analysis of the Chlb region only, which reveals a decay of Chlb fluorescence in 2.3 ps (not shown). Due to the entanglement of these two processes, it is unclear if the 2–3 ps Chlb to Chla transfer component involves transfer either to the bulk or to the red Chla forms (or both). Biphasic Chlb to Chla transfer (in ~ 0.2 – 0.35 ps and 2–3 ps) was, however, also observed in monomers of LHCI¹³ and CP29,¹¹ which do not contain red-shifted Chl's. For CP29 it was shown that the fast Chlb to Chla transfer component corresponds to transfer from the blue-most Chlb form, whereas the slower transfer component occurs from the redmost Chlb form.¹¹ Considering the similarities between CP29 and LHCI, a similar separation of the two (C643 and C650) Chlb to Chla transfer components could be expected in the latter, although our data are not conclusive on this issue.

Equilibration between Bulk Chlorophyll *a* and Red Chlorophyll *a*. Upon 400 nm excitation energy transfer from the bulk Chla's to the red Chla's is found to occur in 8 ps. A separate analysis of parts of the bulk Chla fluorescence decay indicates that the decay time is quite independent of the wavelength. However, upon 465 nm excitation, it is found that the fluorescence decay of bulk Chla's around 675 is faster (4–5 ps) than that of the Chla emission around 685 (7 ps). This

indicates that different pools of bulk Chl a 's may equilibrate with the red Chl's on different time scales varying between 4 and 8 ps.

In addition, a slower bulk Chl a to red Chl a transfer of about 20 ps was observed. Earlier experiments on isolated LHCI showed a 10–45 ps^{5,15,16} and even slower Chl a equilibration components,¹⁶ but did not reveal the faster 4–8 ps equilibration process.

Since it appears that probably all LHCI dimers exhibit a long-wavelength Chl (F730, F702)² (see also below), the observed Chl a equilibration times most probably represent some average of a larger number of equilibration components. If the red-shifted Chl form is assumed to be localized in one of the monomers, the \sim 4–8 ps rates may be interpreted as the intramolecular equilibration within a monomer and the \sim 20 ps rate as intermolecular equilibration between the monomers constituting a dimer. This view is in agreement with recent results by Melkozernov et al.,¹⁷ which show a 4–5 ps Chl a equilibration component present in monomeric reconstituted Lhca4 and reconstituted LHCI-730 heterodimers, whereas a 33 ps equilibration component is present only in the latter. We do note that some mixing of (slow) Chl b to Chl a transfer and Chl a equilibration may have occurred in these experiments as well, since excitation was performed in the Chl b region. In both these and our experiments, the slow (20 ps) bulk to red Chl a energy transfer components are strongly nonconservative, suggesting either that a significant loss of excitations occurs with this time constant or that the acceptor state exhibits a lowered oscillator strength. We can rule out that the observed nonconservativity results from singlet–singlet or singlet–triplet annihilation, considering the conditions under which our experiments were performed. Moreover, a similar nonconservative, slow energy transfer component was observed in pump–probe experiments on CP47 (de Weerd et al., unpublished data). Obviously, if there would be an actual loss of excitations on a tens of picoseconds time scale in LHCI bound to the PSI core complex, this would result in a significant decrease in the light harvesting efficiency of LHCI.

Although LHCII and CP29 do not contain red-shifted Chl a , several equilibration processes were observed in the bulk Chl a band, occurring on subpicosecond and 5–18 ps time scales.^{11,13,14}

Long Lifetimes. Both the 400 and 470 nm excitation data sets reveal two distinct long-lifetime decays of 0.6 and 3 ns. For both wavelengths of excitation the respective spectra of these components appear very similar, with respect to both shape and relative amplitude. In Figure 8 the spectra of the 0.6 and 3 ns components are shown for 470 nm excitation, scaled to their maxima. The 0.6 ns component (solid) peaks a few nanometers red shifted with respect to the 3 ns component (dotted). Although both spectra exhibit a red wing, the wing of the 3 ns component is significantly more pronounced and red shifted than that of the 0.6 ns component. This implies that both “species” possess a different red-shifted Chl a form. This is in agreement with low-temperature experiments by Ihalainen et al.² which reveal a 702 nm emitting species in addition to the established 730–735 nm fluorescence of LHCI. The spectrum of the 3 ns component quite closely resembles the emission spectrum of LHCI-730 reported by Melkozernov et al.⁵ The ratio of the total areas of the 0.6 ns DAS and \sim 3 ns DAS is about 1 to 4. This is quite close to the 1 to 3 ratio which would be expected if one out of four dimers (one Lhca2 homodimer, one Lhca3 homodimer, and two Lhca1/4 heterodimers) has decay properties that are significantly different from those of the other three. It has been suggested that either the Lhca2 or the Lhca3 homo-

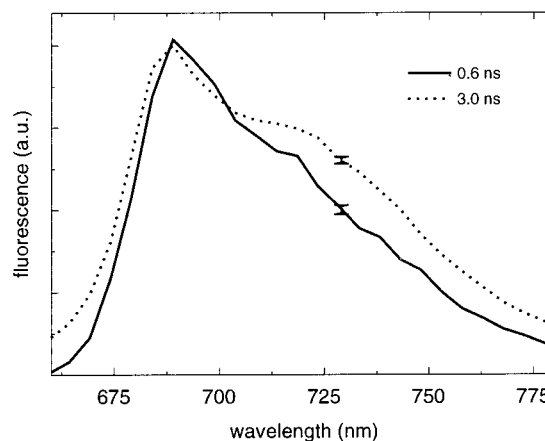


Figure 8. Normalized decay associated spectra of the two slowest components for 470 nm excitation with lifetimes of 0.6 ns (solid) and 3 ns (dotted). Rough error bars have been included at selected wavelengths.

dimer exhibits emission properties similar to those of the Lhca1/Lhca4 heterodimer (i.e., F730), and that the remaining dimer may be responsible for F702 (S. Jansson, personal communication). Therefore, we tentatively assign the 0.6 ns component to a homodimer of either Lhca2 or Lhca3, which at low temperatures may be responsible for the observed F702 fluorescence.

Presently we do not have an exclusive explanation of why the fluorescence decay of this dimer at room temperature is 5-fold faster as compared to the other dimers, since there are several mechanisms that could result in such a shortening of the fluorescence lifetime. Shortening of the fluorescence lifetime has been observed in many (bacterio)chlorophyll containing systems, such as the bacterial light harvesting complexes LH1 and LH2,²⁶ the B820 subunit of LH1,²⁷ the primary electron donor in the bacterial reaction center,^{28,29} and the Chl a in the cytochrome *b_f* complex of *Synechocystis* PCC6803.³⁰ Various explanations have been proposed for the shortening of lifetimes, such as superradiance of the excitonically coupled (B)Chl molecules,²⁶ enhanced internal conversion rates,^{26–28} and quenching of excitations by a nearby amino acid residue.³⁰ It has also been argued that a moderately strong interaction of the Chl Q_y state with the S_1 state of carotenoids can result in a substantial decrease of the fluorescence lifetime.³¹

Melkozernov et al.⁵ observed several long lifetimes in both native and reconstituted LHCI-730, with dominating \sim 300 and \sim 800 ps components. Since these preparations were supposed to consist of the Lhca1/Lhca4 heterodimer only, a single decay lifetime is expected. The observed multiexponential decay must therefore result from some heterogeneity of the sample: possibly the isolation procedures somehow disrupt the sample or maybe some aggregation occurs.

Concluding Remarks: Why Are Red Chl's Found Only in PSI?

The dynamics of LHCI show some remarkable similarities to the light harvesting proteins CP29 and LHCII (see Table 1) of photosystem II. However, photosystem II and its light harvesting proteins do not feature the red-shifted Chl a forms which are found in all PSI core complexes and LHCI. Apparently, in the course of evolution, PSI has experienced a net benefit from the presence of red Chl's, which was not the case for PSII. The cause of this difference may be that PSI is a more efficient photosystem than PSII.^{32,33} A PSI core particle containing no red Chl's is estimated to exhibit a 18 ps effective trapping

time,¹⁹ resulting in a quantum efficiency for charge separation of 99.6% (assuming the rate of losses to be $(5 \text{ ns})^{-1}$). In plant PSI cores the number of red Chl's is small and results in an increase of the effective trapping rate to about 20 ps (Gobets et al., unpublished results). However, in some cyanobacterial PSI cores the number of red Chl's is much larger, resulting in an increase of the effective trapping time of up to 3-fold.¹⁹ Nevertheless, this causes the estimated quantum efficiency to drop by only 0.7%. The quantum efficiency for charge separation of a PSII core particle, which does not contain red Chl's, is only 85%.³² A 3-fold slowdown of the effective trapping rate similar to that in PSI would lead to a 20% decrease of the quantum efficiency in PSII. Clearly, whereas the positive effects of red Chl's (increased red photon absorption, and possibly photoprotection) could easily justify the minute decrease in quantum efficiency in PSI, it is very likely that the large decrease in efficiency in PSII is not compensated by these positive effects.

The relatively low efficiency of PSII is the result of two effects. First of all, energy transfer to the reaction center (RC) is slower in PSII than in PSI. A comparison of the crystal structures of the two photosystems^{34,35} (P. Fromme, personal communication) shows why: in PSI the volume directly surrounding the reaction center is densely packed with about 50 Chl_a molecules, whereas in PSII the same volume is basically empty. Therefore the average distance between the antenna Chl's and the RC is much larger in PSII than in PSI, resulting in a slower transfer to the RC in the former. The reason the volume directly surrounding the RC in PSII is empty may be the risk of damage to the antenna Chl's because of the high redox potential involved in oxygen evolution, as well as the need to be able to easily replace the D1 protein.

The second effect responsible for the low efficiency of PSII is the small energy difference between P680*Pheo and the first charge-separated state P680⁺Pheo⁻, resulting in losses by "delayed fluorescence" due to back-transfer from P680⁺Pheo⁻ to the PSII RC and antenna. The small energy gap is the consequence of tuning the PSII system to obtain the high redox potential, needed for the splitting of water.^{32,36}

Thus, the absence of red Chl's in photosystem II may very well be a direct result of its ability to split water.

Acknowledgment. We thank Claudiu C. Gradinaru for the helpful discussions and suggestions, and Prof. S. Jansson (Umeå) for sharing unpublished work. B.G. was supported with a grant from the Dutch Science Foundation (SIR beurs NWO). J.T.M.K. was supported by the Human Frontier Science Program Organization. J.A.I. was supported with a short-term fellowship from the ESF Program "Biophysics of Photosynthesis". This work was supported by The Netherlands Organization for Scientific Research (NWO) via The Foundation of Earth and Life Sciences (ALW), and by the Director, Office of Science, of the U.S. Department of Energy under Contract No. DE-AC03-76SF00098.

References and Notes

- Jansson, S. *Biochim. Biophys. Acta* **1994**, *1184*, 1.
- Ihalainen, J. A.; Gobets, B.; Sznee, K.; Brazzoli, M.; Croce, R.; Bassi, R.; van Grondelle, R.; Korppi-Tommola, J. E. I.; Dekker, J. P. *Biochemistry* **2000**, *39*, 8625.
- Jansson, S.; Andersen, B.; Scheller, H. V. *Plant Physiol.* **1996**, *112*, 409.
- Schmid, V. H. R.; Cammarata, K. V.; Bruns, B. U.; Schmidt, G. W. *Proc. Natl. Acad. Sci. U.S.A.* **1997**, *94*, 7667.
- Melkozernov, A. N.; Schmid, V. H. R.; Schmidt, G. W.; Blankenship, R. E. *J. Phys. Chem. B* **1998**, *102*, 8183.
- Croce, R.; Bassi, R. In *Photosynthesis: Mechanisms and Effects*; Garab, G., Ed.; Kluwer Academic Publishers: Dordrecht, 1998; p 421.
- Gobets, B.; van Amerongen, H.; Monshouwer, R.; Kruij, J.; Rögner, M.; van Grondelle, R.; Dekker, J. P. *Biochim. Biophys. Acta* **1994**, *1188*, 75.
- Pålsson, L. O.; Dekker, J. P.; Schlodder, E.; Monshouwer, R.; van Grondelle, R. *Photosynth. Res.* **1996**, *48*, 239.
- Boekema, E. J.; Jensen, P. E.; Schlodder, E.; van Breemen, J. F. L.; van Roon, H.; Scheller, H. V.; Dekker, J. P. *Biochemistry* **2001**, *40*, 1039.
- Kühlbrandt, W.; Wang, D. N.; Fujiyoshi, Y. *Nature* **1994**, *367*, 614.
- Gradinaru, C. C.; Pascal, A. A.; van Mourik, F.; Robert, B.; Horton, P.; van Grondelle, R.; van Amerongen, H. *Biochemistry* **1998**, *37*, 1143.
- Gradinaru, C. C.; van Stokkum, I. H. M.; Pascal, A. A.; van Grondelle, R.; van Amerongen, H. *J. Phys. Chem. B* **2000**, *104*, 9330.
- Kleima, F. J.; Gradinaru, C. C.; Calkoen, F.; van Stokkum, I. H. M.; van Grondelle, R.; van Amerongen, H. *Biochemistry* **1997**, *36*, 15262.
- Gradinaru, C. C.; Özdemir, S.; Gülen, D.; van Stokkum, I. H. M.; van Grondelle, R.; van Amerongen, H. *Biophys. J.* **1998**, *75*, 3064.
- Pålsson, L. O.; Tjus, S. E.; Andersson, B.; Gillbro, T. *Biochim. Biophys. Acta* **1995**, *1230*, 1.
- Mukerji, I.; Sauer, K. *Biochim. Biophys. Acta* **1993**, *1142*, 311.
- Melkozernov, A. N.; Lin, S.; Schmid, V. H. R.; Paulsen, H.; Schmidt, G. W.; Blankenship, R. E. *FEBS Lett.* **2000**, *471*, 89.
- Croce, R.; Zucchelli, G.; Garlaschi, F. M.; Jennings, R. C. *Biochemistry* **1998**, *37*, 17355.
- Gobets, B.; van Stokkum, I. H. M.; Rögner, M.; Kruij, J.; Schlodder, E.; Karapetyan, N. V.; Dekker, J. P.; van Grondelle, R. *Biophys. J.* **2001**, *81*, 407.
- Walla, P. J.; Yom, J.; Krueger, B. P.; Fleming, G. R. *J. Phys. Chem. B* **2000**, *104*, 4799.
- Peterman, E. J. G.; Gradinaru, C. C.; Calkoen, F.; Borst, J. C.; van Grondelle, R.; van Amerongen, H. *Biochemistry* **1997**, *36*, 12208.
- Schmid, V. H. R.; Thome, P.; Ruhle, W.; Paulsen, H.; Kuhlbrandt, W.; Rogl, H. *FEBS Lett.* **2001**, *499*, 27.
- Macpherson, A. N.; Gillbro, T. *J. Phys. Chem. A* **1998**, *102*, 5049.
- Polivka, T.; Herek, J. L.; Zigmantas, D.; Akerlund, H. E.; Sundström, V. *Proc. Natl. Acad. Sci. U.S.A.* **1999**, *96*, 4914.
- Kennis, J. T. M.; Gobets, B.; van Stokkum, I. H. M.; Dekker, J. P.; van Grondelle, R.; Fleming, G. R. *J. Phys. Chem. B* **2001**, *105*, 4485.
- Monshouwer, R.; Abrahamsson, M.; van Mourik, F.; van Grondelle, R. *J. Phys. Chem. B* **1997**, *101*, 7241.
- Helenius, V.; Monshouwer, R.; van Grondelle, R. *J. Phys. Chem. B* **1997**, *101*, 10554.
- Breton, J.; Martin, J. L.; Lambry, J. C.; Robles, S. J.; Youvan, D. C. In *Reaction Centers of Photosynthetic Bacteria*; Michel-Beyerle, M. E., Ed.; Springer-Verlag: New York, 1990; p 293.
- van Brederode, M. E.; Jones, M. R.; van Mourik, F.; van Stokkum, I. H. M.; van Grondelle, R. *Biochemistry* **1997**, *36*, 6855.
- Peterman, E. J. G.; Wenk, S. O.; Pullerits, T.; Pålsson, L. O.; van Grondelle, R.; Dekker, J. P.; Rögner, M.; van Amerongen, H. *Biophys. J.* **1998**, *75*, 389.
- van Amerongen, H.; van Grondelle, R. *J. Phys. Chem. B* **2001**, *105*, 604.
- Trissl, H. W.; Wilhelm, C. *Trends Biochem. Sci.* **1993**, *18*, 415.
- van Grondelle, R.; Dekker, J. P.; Gillbro, T.; Sundström, V. *Biochim. Biophys. Acta* **1994**, *1187*, 1.
- Krauss, N.; Schubert, W. D.; Klukas, O.; Fromme, P.; Witt, H. T.; Saenger, W. *Nat. Struct. Biol.* **1996**, *3*, 965.
- Zouni, A.; Witt, H. T.; Kern, J.; Fromme, P.; Krauss, N.; Saenger, W.; Orth, P. *Nature* **2001**, *409*, 739.
- Diner, B. A.; Babcock, G. T. In *Oxygenic Photosynthesis: The Light Reactions*; Ort, D. R., Yocum, C. F., Eds.; Kluwer Academic Publishers: Dordrecht, 1996; p 213.